

## Article

# High-Reliability Perovskite Quantum Dots Using Atomic Layer Deposition Passivation for Novel Photonic Applications

Tzu-Yi Lee <sup>1,†</sup>, Tsau-Hua Hsieh <sup>2,3,†</sup>, Wen-Chien Miao <sup>4,†</sup>, Konthoujam James Singh <sup>1</sup>, Yiming Li <sup>3</sup> , Chang-Ching Tu <sup>4</sup>, Fang-Chung Chen <sup>1,\*</sup> , Wen-Chung Lu <sup>5</sup> and Hao-Chung Kuo <sup>1,4,\*</sup> 

<sup>1</sup> Department of Photonics, College of Electrical and Computer Engineering, National Yang Ming Chiao Tung University, Hsinchu 30010, Taiwan

<sup>2</sup> Technology Development Center, InnoLux Corporation, Hsinchu 35053, Taiwan

<sup>3</sup> Institute of Communications Engineering, College of Electrical and Computer Engineering, National Yang Ming Chiao Tung University, Hsinchu 30010, Taiwan

<sup>4</sup> Semiconductor Research Center, Hon Hai Research Institute, Taipei 11492, Taiwan

<sup>5</sup> Executive Office, SkyTech Institute, Hsinchu 303, Taiwan

\* Correspondence: fcchendop@nycu.edu.tw (F.-C.C.); hckuo@faculty.nctu.edu.tw (H.-C.K.)

† These authors contributed equally to this work.

**Abstract:** In this study, we propose highly stable perovskite quantum dots (PQDs) coated with Al<sub>2</sub>O<sub>3</sub> using atomic layer deposition (ALD) passivation technology. This passivation layer effectively protects the QDs from moisture infiltration and oxidation as well as from high temperatures and any changes in the material characteristics. They exhibit excellent wavelength stability and reliability in terms of current variation tests, long-term light aging tests, and temperature/humidity tests (60°/90%). A white-light system has been fabricated by integrating a micro-LED and red phosphor exhibiting a high data transmission rate of 1 Gbit/s. These results suggest that PeQDs treated with ALD passivation protection offer promising prospects in full-color micro-displays and high-speed visible-light communication (VLC) applications.

**Keywords:** ALD passivation technology; perovskite quantum dots; reliability; micro-displays; VLC



**Citation:** Lee, T.-Y.; Hsieh, T.-H.; Miao, W.-C.; James Singh, K.; Li, Y.; Tu, C.-C.; Chen, F.-C.; Lu, W.-C.; Kuo, H.-C. High-Reliability Perovskite Quantum Dots Using Atomic Layer Deposition Passivation for Novel Photonic Applications. *Nanomaterials* **2022**, *12*, 4140. <https://doi.org/10.3390/nano12234140>

Academic Editor: Yurii K. Gun'ko

Received: 27 October 2022

Accepted: 21 November 2022

Published: 23 November 2022

**Publisher's Note:** MDPI stays neutral with regard to jurisdictional claims in published maps and institutional affiliations.



**Copyright:** © 2022 by the authors. Licensee MDPI, Basel, Switzerland. This article is an open access article distributed under the terms and conditions of the Creative Commons Attribution (CC BY) license (<https://creativecommons.org/licenses/by/4.0/>).

## 1. Introduction

Quantum dots (QDs) have received a lot of attention in recent years as one of the prospective light emitters for wide color gamut displays that can effectively meet the demands for a conveniently tunable wavelength, high efficiency, process reliability, operating stability, and color purity [1–4]. The excellent facile and economical solution processability of colloidal QDs makes it possible to integrate inorganic semiconductors into high-performance and flexible device architectures. Because of their exceptional qualities, including their narrow emission bandwidth, high fluorescent quantum yield, tunable emission color, and wide color gamut, QDs are the leading candidate for the field of next-generation solid-state lighting and displays. QDs have recently gained considerable interest as a promising contender for a wide variety of optoelectronic applications, including light-emitting diodes (LED) [1,5], solar cells [6,7], photodetectors [8], lasers [9], photocatalysis [10], biomedical imaging [11], lighting [12], and visible-light communication (VLC) [13,14]. The commercialization of QDs in the display sector is attributed, in particular, to conventional CdSe QDs from the II-VI group, which exhibit a high photoluminescence quantum yield (PLQY) in addition to other exceptional optical properties. With tremendous success, Cd QD-based LEDs have achieved significant advancements in their ability to serve as either the active layer or color conversion layer in EL devices. However, Cd-based QDs have a limited potential for use in commercial LEDs due to their toxicity and health risks, which raises some environmental concerns when it comes to mass manufacturing for commercial use. As a result, the development of environmentally friendly counterparts has long been a crucial requirement for the future generation of displays.

Perovskite quantum dots (PQDs) are a viable contender as a replacement for Cd-based QDs in next-generation display technology owing to their near-unity PLQY, narrow emission, high quantum yield, tunable emission spectra, and short radiative lifetime. Furthermore, the mid-gap trap states are not significantly impacted by the dangling bonds on the surfaces of PQDs, which is extremely advantageous for effective radiative emissions [1–4]. It has been conclusively demonstrated that it is possible to optimize a variety of useful optical properties of PQDs, including emission wavelengths, optical absorption, long carrier diffusion lengths [15,16], and high carrier mobility [17,18], using a variety of techniques, including a straightforward ligand-mediated approach. As a result, the distinct optoelectronic properties of PQDs and their simple synthetic methods enable unprecedented advancements in contemporary optoelectronic and photovoltaic systems. Recently, PQDs have gained a considerable amount of interest in VLC applications owing to their short carrier lifetime [14,19]. There have been numerous reports on PQDs realizing white-light systems by integrating blue micro-LEDs, achieving a high modulation bandwidth for VLC [13,14]. However, PQDs typically experience considerable issues with chemical, optical, or thermal instability induced by their ionic structure and large surface energy; hence, long-term stability continues to be a barrier to their usage on an industrial scale [20,21]. Additionally, when it comes to on-chip QD LEDs, the high energy radiation from blue LEDs might cause the thermal quenching and photodegradation of PQDs, which limits their practical application. Due to these challenges, on-chip PQD LEDs have substantially lower luminous efficiency than conventional phosphor-based LEDs. As a result, increasing the stability of PQDs has become a prominent topic in recent research to extend the lifetime of QDs. Over the past few years, a number of techniques have been proposed to improve the stability of PQDs, including codoping or hybridizing with other cations, surface passivation, and so on [6,7,22].

Another approach to enhancing PQD stability is encapsulation, which involves coating or isolating the PQDs with the introduction of layers of stable organic molecules or an inorganic matrix that is both airtight and mechanically robust. Effective encapsulations can increase their resistance to oxygen or humidity by isolating PQDs from one another using an additional matrix [13,23–29]. In particular, the encapsulating technique may effectively protect PQDs from agglomeration in the solution and prevent anion exchange when the PQDs are mixed with various halide compositions. It can also reduce degradation when subjected to polar solvents, harsh environments, high-energy radiation, and high temperatures. The coating methods and materials commonly used today include polymers, SiO<sub>2</sub>, Al<sub>2</sub>O<sub>3</sub>, covalent organic frameworks (COF), etc. However, polymer and SiO<sub>2</sub> coatings often require the use of highly polarized solvents [30–32]. After the coating is completed, the reliability can be improved, but the PLQY will decrease more. Al<sub>2</sub>O<sub>3</sub> is mostly used in CsPbBr<sub>3</sub> PQD LED devices [33,34]. The ALD passivation protection technique is used to grow a thin layer of Al<sub>2</sub>O<sub>3</sub> on the QD element, but due to the insulating nature of Al<sub>2</sub>O<sub>3</sub>, the thick intermediate layer will block the QD element. However, due to the insulating nature of Al<sub>2</sub>O<sub>3</sub>, an excessively thick intermediate layer can block electron transfer. Therefore, the thickness is limited. COF is an advanced class of highly crystalline porous polymeric materials that are often used as photocatalysts for solar photovoltaic applications [35,36]. In addition to this, atomic layer deposition (ALD) is also a promising approach to forming inorganic matrices or coatings to encapsulate QDs. Studies have demonstrated that ALD growth can protect QDs against environmental degradation, oxidation, ripening, and sintering [37,38]. Moreover, ALD growth can enhance the performance of QDs and QD layers, which will result in increased charge carrier mobility and charge carrier multiplication [1,5,39]. As a result, the ALD process has enormous potential as a method for post-functionalizing QDs in addition to encapsulating and protecting them from oxidation. In this work, we developed a novel approach to the Al<sub>2</sub>O<sub>3</sub> capping of PQDs by using ALD. The experimental results show that Al<sub>2</sub>O<sub>3</sub> capping can indeed improve reliability while maintaining efficiency.

## 2. Materials and Methods

In this study, a PQD film with high reliability was developed. First, see Chen et al.'s synthesis of FAPbBr<sub>3</sub> QDs [40]. FAPbBr<sub>3</sub> QDs were synthesized using the ligand-assisted re-precipitation (LARP) method at room temperature [40,41]. First of all, 500 µL of oleic acid (OA), 0.16 mmol formamidinium bromide (FABr), 0.2 mmol lead (II) iodide (PbBr<sub>2</sub>), and 20 µL of octylamine were mixed. After thoroughly mixing, 10 mL of toluene was gently added and stirred for 5 min, and then 5 mL of acetonitrile was added, followed by mixing uniformly. High-speed centrifugation was used to separate the mixture in the solution for 25 min at 6000 rpm, after which the supernatant was removed, and the pellet was then dissolved in 10 mL of toluene. After uniform mixing, 30 µL of an excess-lead-ion solution formed by mixing 1.512 mmol PbBr<sub>2</sub>, propionic acid, butylamine, and n-hexane was added. Then, 500 µL of OA and 10 mL of methyl acetate were added to the solution, allowed to react for 5 min, and then centrifuged for 25 min at 8000 rpm. After removing the supernatant, the pellet was once again dissolved in 5 mL of toluene and centrifuged at 8000 rpm for a further 15 min. Finally, a clear green liquid, i.e., the FAPbBr<sub>3</sub> PQD solution, was collected, which was ready for post-synthesis surface optimization [42,43]. Next, the Atomila GT atomic layer powder spraying equipment developed by SkyTech Institute (Hsinchu, Taiwan) was used to coat the surfaces of PQDs with Al<sub>2</sub>O<sub>3</sub> to realize the passivation protection of PQDs. A protective layer of Al<sub>2</sub>O<sub>3</sub> was deposited on PQDs using trimethylaluminum (Al(CH<sub>3</sub>)<sub>3</sub>, TMA) and ozone (O<sub>3</sub>) as precursors and water as a co-reactant at 150 °C for 200 cycles (deposition rate: 2.5 Å/cycle), and the resulting sample is named PeQD. The ALD equipment developed by SkyTech Institute has a special powder "dust flow field" design with a cavity that can rotate 360 degrees to generate a uniform powder flow field. It is different from the previous plating on the surface of the QD film with a protective layer [39,44–48]. The method proposed in this study can improve the application degree of QDs. Finally, we mixed PeQDs, KSF red phosphor, nanoscale TiO<sub>2</sub> scattering particles, dispersant, and UV glue uniformly for PeQD thin-film preparation. The mixture was poured into a model, and air bubbles were removed from it using a vacuum pumping system. Finally, UV light was irradiated to cure it, and then the PeQD thin film was formed.

## 3. Results and Discussion

### 3.1. Surface Topography Analysis

The instability of PQDs' surface bonding is well understood. When QDs are subjected to external stimuli, such as light, hot water, oxygen, etc., the surface ligands are easily peeled off, resulting in the phenomenon of fluorescence quenching and causing a significant drop in the photoluminescence quantum yield (PLQY) [49,50]. This study referred to Chen et al.'s ligand-assisted re-precipitation (LARP) method for synthesizing QDs [40]. The aggregation phenomena of QDs and surface defects of QDs induced by the dissolution crystallization method were monitored using post-synthesis optimization processing technology. In this method, excess Br<sup>-</sup> is added to the purified FAPbBr<sub>3</sub> QD solution to make up for the vacancy of halogen anions generated during the purification process and to increase the bonding strength between the ligand and the QD surface [42]. Then, the ALD passivation protection technology is used to coat the surfaces of the PQDs with oxides, which are named PeQDs. This passivation layer not only protects the QDs from high temperatures and any changes in material properties but also protects the QDs from moisture and oxidation. This is an effective passivation method at present, and a schematic diagram is shown in Figure 1a. Figure 1b shows a comparison of the optical properties of post-synthesis optimization processing technology and ALD passivation protection technology. PeQDs and PQDs have wavelengths, full width at half maximum (FWHM) values, and PLQYs of 525, 25 nm, and 99% and 525, 25 nm, and 78%, respectively. After applying ALD passivation protection technology, there is a slight decrease in the PLQY part. This is attributed to the addition of water and high temperature during the coating process. Figure 1c shows the XRD analysis. It can be observed in the figure that the PeQDs do not produce any phase changes,

indicating that the ALD passivation protection technology does not affect the QD structure. Figure 1d,e present the TEM images of  $\text{Al}_2\text{O}_3$  coated on the surfaces of PeQDs. The gray portion in the figure is the  $\text{Al}_2\text{O}_3$  matrix, and the darker spots correspond to PeQDs, which is confirmed by the mapping analysis shown in Figure 1f. The ALD passivation technology developed in this study was used to coat the surfaces of PeQDs with  $\text{Al}_2\text{O}_3$ , which can effectively isolate the influence of water vapor and oxygen, thereby improving reliability.

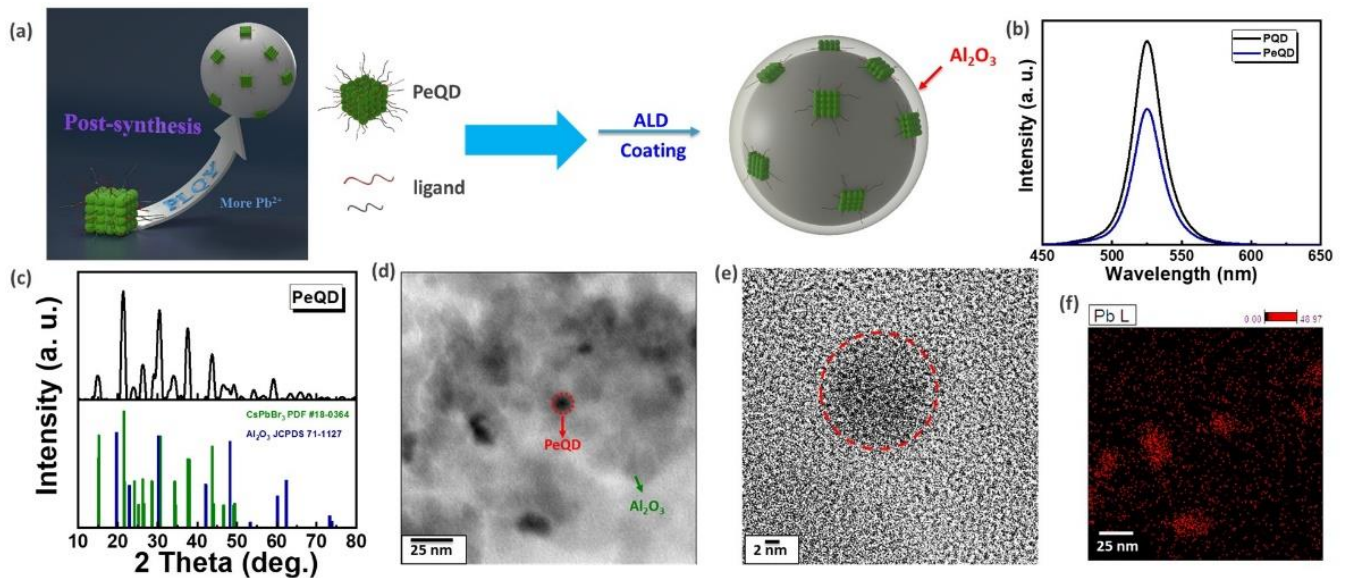


**Figure 1.** Surface topography analysis of PeQDs. (a) Schematic diagram of surface modification. (b) Spectra of PQDs and PeQDs. (c) XRD image. (d) TEM image. (e) High-magnification TEM image. (f) Mapping analysis image.

### 3.2. Optical Characterization Analysis

Green PeQDs treated with ALD passivation were uniformly mixed with UV glue to make composite films, and their optical characteristics were evaluated. Figure 2a,b show the optical illumination from the PeQD composite film under UV light and blue LED exposure, respectively, showing a bright green-colored light. The PeQD film under 446 nm blue LED exposure exhibits an emission wavelength of 525 nm, an FWHM of 25 nm, and a PLQY of 45%. As shown in Figure 2c, PLQY is defined as the ratio of the emitted photons to the absorbed photons as follows [51]:

$$\text{PLQY} = \frac{\text{Emission}}{\text{Absorbance}} = \frac{\# \text{ of excited green photons}}{\# \text{ of absorbed blue photons}} \quad (1)$$

The driving current for the blue LED was changed from 1 to 70 mA in order to test the reliability of the PeQD film. Figure 2d,e illustrate spectrograms and the Commission Internationale de l'Éclairage (CIE) color coordinates of the PeQD film, respectively, with a varying driving current. It can be seen that the  $\text{Al}_2\text{O}_3$  layer can indeed effectively protect PeQDs from the high radiation of the blue LED illumination. With the increasing current, the CIE color coordinates are slightly shifted from (0.147, 0.803) to (0.163, 0.781), with no emission wavelength shift. The PeQD film exhibits a maximum luminous efficiency of 130.4 lm/W at a current density of  $7.48 \times 10^{-3} \text{ A/cm}^2$  (10 mA) and a minimum luminous efficiency of 112 lm/W at a current density of  $7.48 \times 10^{-4} \text{ A/cm}^2$  (1 mA), as shown in Figure 2f. EQE is defined as the ratio of the number of photons emitted into free space per second to the number of electrons injected into the LED per second, where  $P_0$  is the radiant

power (coupled to free space),  $h\nu$  is the photon energy,  $I$  is the injection current, and  $e$  is the fundamental charge, and is calculated as follows [52]:

$$\text{EQE} = \frac{\text{Emitted photons outside LED}/s}{\text{Input electrons}/s} = \frac{P_0 / h\nu}{I / e} \quad (2)$$

The external quantum efficiency (EQE) of the PeQD film is 37.0%, as shown in Figure 2g, showing an EQE stability as a function of current density. The experimental results confirmed that the green PeQD film treated with ALD passivation protection can effectively improve reliability. In addition, the PeQD film displayed no emission wavelength shifts with the changing current and excellent light-emitting characteristics, which is promising for future optical applications.

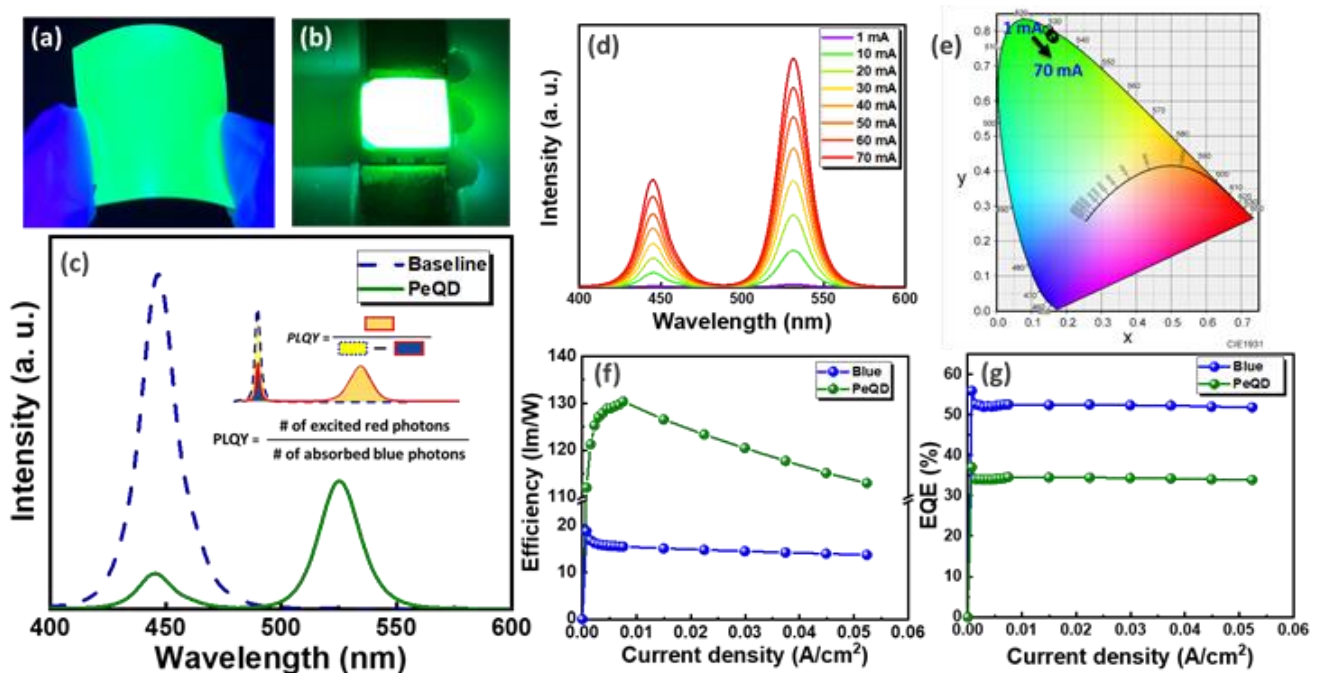


**Figure 2.** Optical properties of green PeQD film. (a) UV lamp, (b) light color image of blue LED excitation. (c) Emission spectrum (20 mA). Current variation test (1–20 mA) (d) emission spectrum image, (e) CIE color coordinates, (f) luminous efficiency, and (g) EQE.

With the research findings in the above section, it is essential to develop white-light components to increase the potential application of green-light PeQD powders. The PeQDs were uniformly mixed with KSF red phosphors having an emission wavelength of 630 nm and UV glue and then excited by blue LEDs (446 nm) to make white LEDs. This strategy, however, is ineffective since the reabsorption effect is caused by the self-aggregation of the nanoscale PeQD powder [5,24,29,53]. The light scattering is enhanced by adding a light scatterer, i.e.,  $\text{TiO}_2$  nanoparticles, to the mixture. By mixing  $\text{TiO}_2$  nanoparticles in PeQDs, KSF red phosphor, and UV glue, the optical path direction of blue light can be increased and can become randomized, thereby increasing the absorption of blue light by PeQDs [23,24,54] and improving the light conversion efficiency (LCE) of PeQDs. A schematic diagram for the composite film consisting of PeQDs,  $\text{TiO}_2$ , and red phosphor is shown in Figure 3a. Figure 3b,c show the optical images of the white-light devices with and without illumination. Figure 3d,e show the emission spectrum and CIE color coordinates of the white-light device with the increasing current. The emission spectra of the white-light device, including the three primary colors, R, G, and B, exhibit no wavelength shifts with an increase in current. The chromaticity coordinates of the device are only slightly shifted from (0.34, 0.31) to (0.34, 0.30). This is because the surfaces of PeQDs are fully passivated

with ALD technology, which can effectively mitigate the impact of light radiation and significantly increase reliability, which is highly beneficial for market demands.

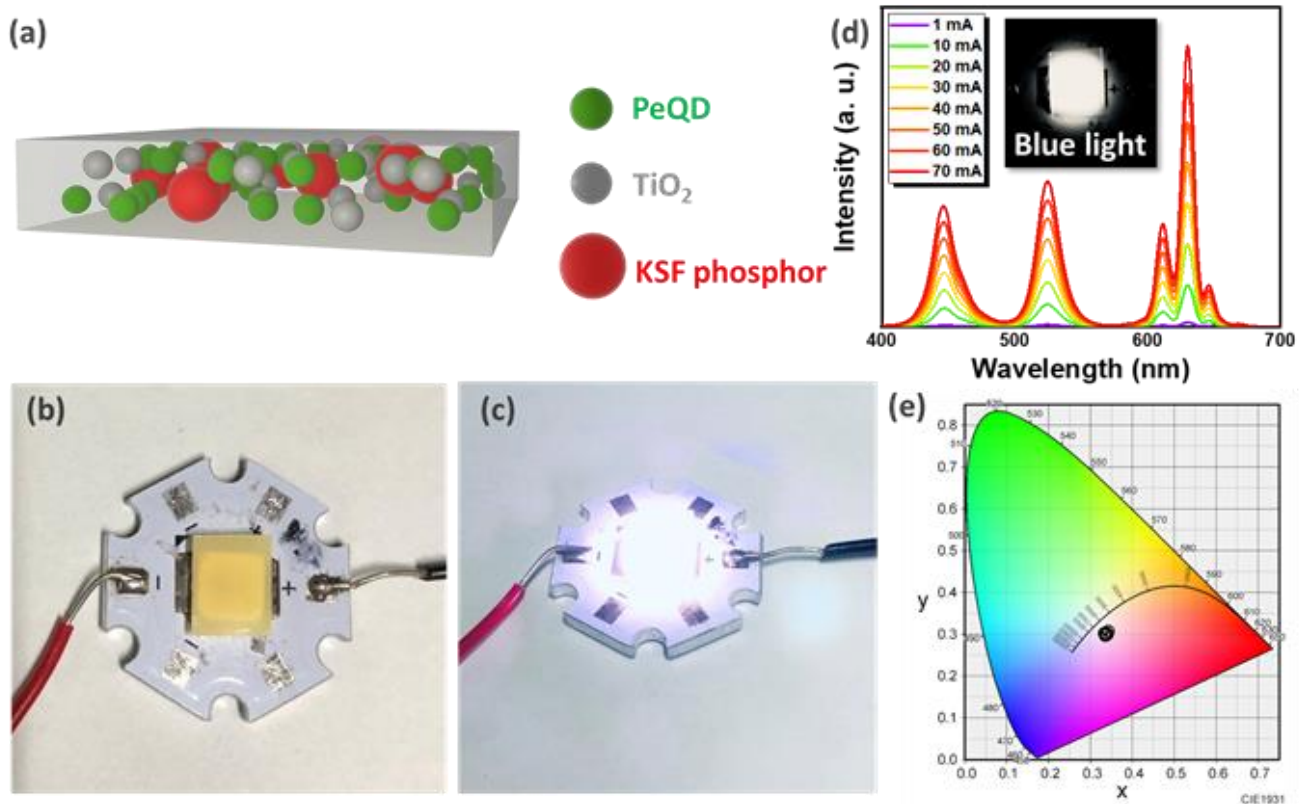


**Figure 3.** Optical properties of white PeQD composite film. (a) Schematic image of film formation. (b,c) Optical image of white-light LED (20 mA) with and without illumination. Current variation test (d) emission spectrogram and (e) CIE color coordinates.

### 3.3. Reliability

Although PQDs have excellent optical properties, the reliability issue is the key to their application. To significantly enhance their PLQY, PeQDs first undergo post-synthesis optimization processing technologies to passivate PeQD surface defects. Then, ALD passivation technology is introduced to protect the QDs from oxidation, moisture, high temperatures, and any changes in the material characteristics. Figure 4a shows the reliability test of the white PeQD composite film, where the long-term lighting test was carried out using a blue LED, with the current being fixed at 20 mA. It was found that after long-term lighting for 1100 h, the PLQY only dropped to the original 0.225 compared with PQD films without ALD passivation protection treatment. Due to the lack of  $\text{Al}_2\text{O}_3$  protection, the original PLQY of the PQD film was reduced to 13%. After the long-term aging test, the PLQY of PQDs was lower than the original 50% within 12 h. This shows that ALD passivation protection technology can effectively improve the reliability of QD films. In order to properly assess the long-term lighting lifetime of a component, a criterion called LT50 can be linearly extrapolated from the last 1100 h of data, defined as the lifetime to 50% of its initial value, and 50% of the initial peak intensity is calculated as follows [29]:

$$\text{LT50} = \frac{(50 - \text{intercept})}{\text{slope}} \quad (3)$$

where the slope and intercept are linear fit parameters to the data we obtained during the successive aging of each device.

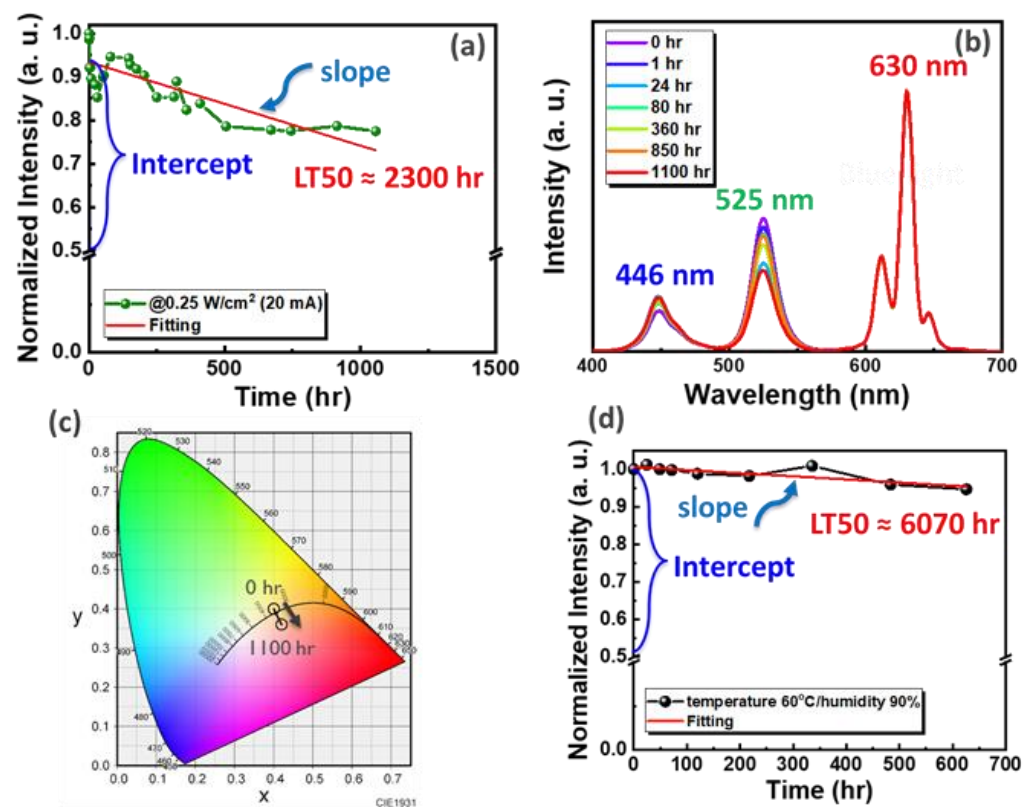


**Figure 4.** Reliability test of white PeQD composite film. White PeQD composite film (20 mA) excited with blue light: (a) decay trend image, (b) emission spectrum, and (c) CIE color coordinates. (d) Aging test at 60°/90%.

The long-term lighting reliability spectrum is shown in Figure 4b. Its CIE color coordinates are shifted from (0.40, 0.40) to (0.42, 0.36), as shown in Figure 4c, showing excellent reliability. In order to explore the influence of temperature and humidity on PeQDs, a long-term test with temperature and humidity of 60°/90% was carried out, and after 624 h, the attenuation was only 0.053, as shown in Figure 4d. These results indicate that ALD passivation technology can effectively protect QDs from high temperatures and any changes in material properties and protect QDs from moisture and oxidation.

### 3.4. Visible-Light Communication (VLC)

In order to create efficient full-color displays and white LEDs for high-speed visible-light communication, it has become increasingly common in recent years to integrate micro-LEDs and colloidal QDs as color conversion layers. The VLC application architecture image is shown in Figure 5a [55]. We used a 30  $\mu\text{m}$  sized micro-LED array as the light source in the data transmission experiment, as shown in Figure 5b. Figure 5c shows the data transmission characteristics of a blue micro-LED combined with the white PeQD composite film analyzed by an on-off keying (OOK) system. The test bit sequence is a non-return-to-zero (NRZ)  $2^7-1$  pseudo-random binary sequence (PRBS7) generated by a bit pattern generator (Anritsu MP1800A). The frequency response of the white PeQD composite film and  $\mu\text{LED}$  was measured after being passed through an optical filter, and the  $-3$  dB bandwidth was 500 MHz at an injection current of 10 mA (current density of 35  $\text{A}/\text{cm}^2$ ). Figure 5d shows the detected NRZ-OOK eye diagram showing a clear opening of the eye diagram at 1 Gbit/s, indicating the potential application of the micro-LED combined with the white PeQD composite film for high-speed VLC applications.

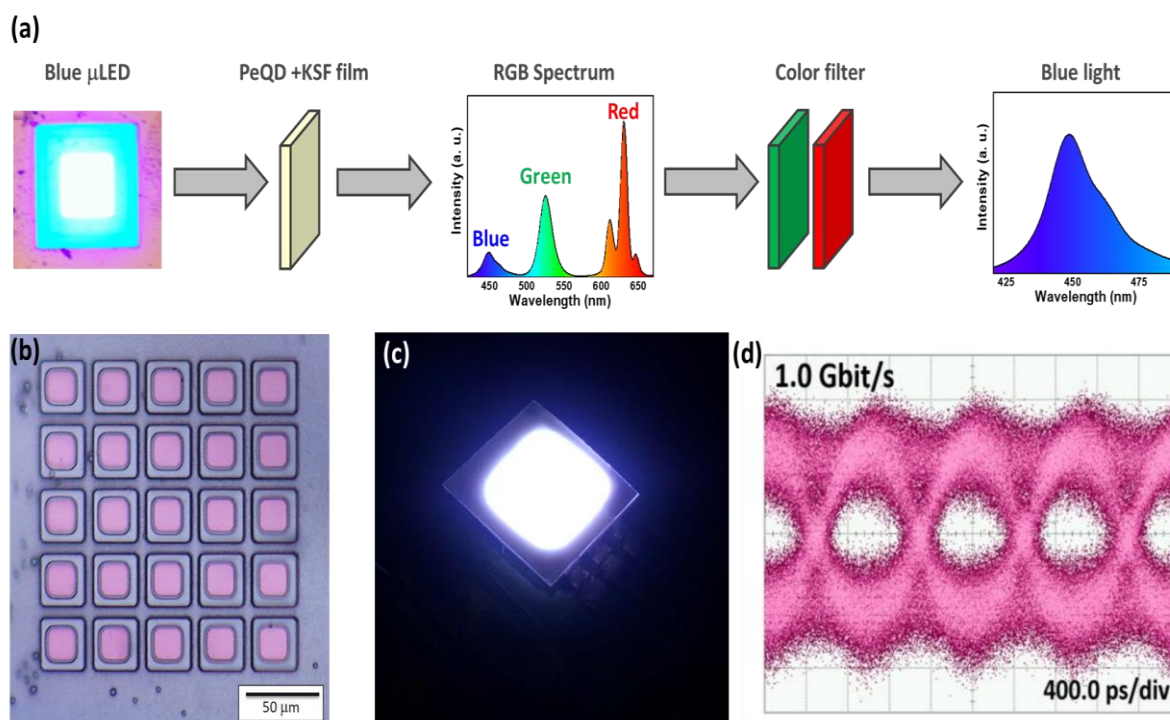


**Figure 5.** White PeQD composite film VLC application. (a) Architecture image. (b) Optical microscope (OM) image of 50  $\mu\text{m}$  micro-LED. (c) Light color diagram of blue micro-LED combined with white PeQD composite film. (d) Detected NRZ-OOK eye diagram at 1 Gbit/s.

#### 4. Conclusions

In summary, we demonstrate a technique for coating oxides on the surfaces of QDs using ALD passivation protection technology. With this method, QDs can be effectively protected from high temperatures and any changes in material properties and can also be protected from moisture and oxidation. The PeQDs exhibit significant wavelength stability with a change in current. The green PeQD film treated with ALD passivation has a maximum luminous efficiency of 130.4 lm/W. Green PeQDs, KSF red phosphors, and dispersive  $\text{TiO}_2$  particles were mixed into the process film, and the blue LED was used to excite the composite film to make a white LED. After 1100 h of the long-term aging test, the efficiency only dropped to the original 0.225 with an LT50 of about 2300 h, and for the 60°/90% temperature/humidity test, LT50 was about 6070 h. The white-light device made by using the PeQD composite film exhibited a high data transmission rate of 1 Gbit/s. These results suggest that PeQDs protected by ALD passivation are very promising for full-color display and VLC applications.

**Author Contributions:** T.-Y.L., T.-H.H. and W.-C.M. contributed equally to this work. Conceptualization, T.-Y.L. and H.-C.K.; Methodology, Y.L., C.-C.T., F.-C.C. and H.-C.K.; Software, T.-Y.L. and W.-C.M.; Validation, K.J.S. and T.-H.H.; Investigation, T.-Y.L.; Resources, W.-C.L., F.-C.C. and H.-C.K.; Data Management, T.-Y.L. and T.-H.H.; Writing—Manuscript Preparation, T.-Y.L. and W.-C.M.; Writing—Commenting and Editing, T.-Y.L. and K.J.S.; Visualization, K.J.S.; Supervision, C.-C.T., W.-C.L., F.-C.C. and H.-C.K.; Project Management, F.-C.C. and H.-C.K.; Funding Acquisition, F.-C.C. and H.-C.K. All authors have read and agreed to the published version of the manuscript.

**Funding:** We are grateful for the financial support provided by the National Science and Technology Council of Taiwan under contract nos. NSTC 111-2622-E-A49 -014 -, 111-2124-M-A49 -004 -, and 108-2221-E-009-113-MY3.

**Acknowledgments:** We thank SkyTech Institute for providing the quantum dot ALD passivation protection technology.

**Conflicts of Interest:** The authors declare no conflict of interest.

## References

1. Liu, Z.; Lin, C.-H.; Hyun, B.-R.; Sher, C.-W.; Lv, Z.; Luo, B.; Jiang, F.; Wu, T.; Ho, C.-H.; Kuo, H.-C.; et al. Micro-Light-Emitting Diodes with Quantum Dots in Display Technology. *Light Sci. Appl.* **2020**, *9*, 83. [[CrossRef](#)] [[PubMed](#)]
2. Shirasaki, Y.; Supran, G.J.; Bawendi, M.G.; Bulović, V. Emergence of Colloidal Quantum-Dot Light-Emitting Technologies. *Nat. Photonics* **2013**, *7*, 13–23. [[CrossRef](#)]
3. Zhu, R.; Luo, Z.; Chen, H.; Dong, Y.; Wu, S.-T. Realizing Rec. 2020 color gamut with quantum dot displays. *Opt. Express* **2015**, *23*, 23680–23693. [[CrossRef](#)] [[PubMed](#)]
4. Zhu, S.; Song, Y.; Wang, J.; Wan, H.; Zhang, Y.; Ning, Y.; Yang, B. Photoluminescence mechanism in graphene quantum dots: Quantum confinement effect and surface/edge state. *Nano Today* **2017**, *13*, 10–14. [[CrossRef](#)]
5. Lin, Y.; Fan, X.; Yang, X.; Zheng, X.; Huang, W.; Shangguan, Z.; Wang, Y.; Kuo, H.-C.; Wu, T.; Chen, Z. Remarkable Black-Phase Robustness of CsPbI<sub>3</sub> Nanocrystals Sealed in Solid SiO<sub>2</sub>/AlO<sub>x</sub> Sub-Micron Particles. *Small* **2021**, *17*, 2103510. [[CrossRef](#)]
6. Wu, T.-H.; Sharma, G.D.; Chen, F.-C. Surface-Passivated Single-Crystal Micro-Plates for Efficient Perovskite Solar Cells. *Processes* **2022**, *10*, 1477. [[CrossRef](#)]
7. Kuo, C.-C.; Sharma, G.D.; Chen, F.-C. p-doping the interfacial layers with tetrakis (pentafluorophenyl) borate improves the power conversion efficiencies in single-crystal perovskite solar cells. *Surf. Interfaces* **2022**, *30*, 101858. [[CrossRef](#)]
8. Li, H.; Li, Z.; Liu, S.; Li, M.; Wen, X.; Lee, J.; Lin, S.; Li, M.-Y.; Lu, H. High performance hybrid MXene nanosheet/CsPbBr<sub>3</sub> quantum dot photodetectors with an excellent stability. *J. Alloy. Compd.* **2022**, *895*, 162570. [[CrossRef](#)]
9. Zhan, W.; Meng, L.; Shao, C.; Wu, X.-g.; Shi, K.; Zhong, H. In Situ Patterning Perovskite Quantum Dots by Direct Laser Writing Fabrication. *ACS Photonics* **2021**, *8*, 765–770. [[CrossRef](#)]
10. Shu, M.; Zhang, Z.; Dong, Z.; Xu, J. CsPbBr<sub>3</sub> Perovskite Quantum Dots Anchored on Multiwalled Carbon Nanotube For Efficient CO<sub>2</sub> Photoreduction. *Carbon* **2021**, *182*, 454–462. [[CrossRef](#)]
11. Wang, A.; Muhammad, F.; Liu, Y.; Deng, Z. Lead-Free Mn-Doped Antimony Halide Perovskite Quantum Dots with Bright Deep-Red Emission. *Chem. Commun.* **2021**, *57*, 2677–2680. [[CrossRef](#)] [[PubMed](#)]
12. Su, C.-Y.; Wu, Y.-C.; Cheng, C.-H.; Wang, W.-C.; Wang, H.-Y.; Chen, L.-Y.; Kuo, H.-C.; Lin, G.-R. Color-Converting Violet Laser Diode with an Ultrafast BEHP-PPV + MEH-PPV Polymer Blend for High-Speed White Lighting Data Link. *ACS Appl. Electron. Mater.* **2020**, *2*, 3017–3027. [[CrossRef](#)]
13. Wu, T.; Lin, Y.; Huang, Y.-M.; Liu, M.; Singh, K.J.; Lin, W.; Lu, T.; Zheng, X.; Zhou, J.; Kuo, H.-C.; et al. Highly Stable Full-Color Display Device with VLC Application Potential Using Semipolar  $\mu$ LEDs and All-Inorganic Encapsulated Perovskite Nanocrystal. *Photonics Res.* **2021**, *9*, 2132–2143. [[CrossRef](#)]
14. Singh, K.J.; Fan, X.; Sadhu, A.S.; Lin, C.-H.; Liou, F.-J.; Wu, T.; Lu, Y.-J.; He, J.-H.; Chen, Z.; Wu, T.; et al. CsPbBr<sub>3</sub> perovskite quantum-dot paper exhibiting a highest 3 dB bandwidth and realizing a flexible white-light system for visible-light communication. *Photonics Res.* **2021**, *9*, 2341–2350. [[CrossRef](#)]
15. Ning, Z.; Gong, X.; Comin, R.; Walters, G.; Fan, F.; Voznyy, O.; Yassitepe, E.; Buin, A.; Hoogland, S.; Sargent, E.H. Quantum-Dot-In-Perovskite Solids. *Nature* **2015**, *523*, 324–328. [[CrossRef](#)]
16. Chouhan, L. An Investigation of Single-Particle Photoluminescence Blinking in Halide Perovskite Nanocrystals and Quantum Dots. Ph.D. Thesis, Hokkaido University, Sapporo, Japan, 2021.
17. Bi, C.; Kershaw, S.V.; Rogach, A.L.; Tian, J. Improved stability and photodetector performance of CsPbI<sub>3</sub> perovskite quantum dots by ligand exchange with aminoethanethiol. *Adv. Funct. Mater.* **2019**, *29*, 1902446. [[CrossRef](#)]
18. Zhou, S. Rapid separation and purification of lead halide perovskite quantum dots through differential centrifugation in nonpolar solvent. *RSC Adv.* **2021**, *11*, 28410–28419. [[CrossRef](#)]
19. Liu, Z.; Hyun, B.-R.; Sheng, Y.; Lin, C.-J.; Changhu, M.; Lin, Y.; Ho, C.-H.; He, J.-H.; Kuo, H.-C. Micro-Light-Emitting Diodes Based on InGaN Materials with Quantum Dots. *Adv. Mater. Technol.* **2022**, *7*, 2101189. [[CrossRef](#)]
20. Wen, Z.; Xie, F.; Choy, W.C. Stability of Electroluminescent Perovskite Quantum Dots Light-Emitting Diode. *Nano Sel.* **2022**, *3*, 505–530. [[CrossRef](#)]
21. Xu, J.; Ma, J.; Gu, Y.; Li, Y.; Li, Y.; Shen, H.; Zhang, Z.; Ma, Y. Progress of Metal Halide Perovskite Crystals From a Crystal Growth Point of View. *Cryst. Res. Technol.* **2022**, 2200128. [[CrossRef](#)]
22. Bhosale, S.S.; Jokar, E.; Chiang, Y.-T.; Kuan, C.-H.; Khodakarami, K.; Hosseini, Z.; Chen, F.-C.; Diau, E.W.-G. Mn-Doped Organic-Inorganic Perovskite Nanocrystals for a Flexible Luminescent Solar Concentrator. *ACS Appl. Energy Mater.* **2021**, *4*, 10565–10573. [[CrossRef](#)]
23. Huang, S.-K.; Weng, S.-Y.; Lee, G.-Y.; Huang, Y.-M.; Kuo, H.-C.; Lin, C.-C. An Investigation on High-Resolution Color Conversion Layer Based on Colloidal Quantum Dots. In Proceedings of the CLEO: Applications and Technology, San Jose, CA, USA, 15–20 May 2022; p. JW3B.182.
24. Hyun, B.-R.; Sher, C.-W.; Chang, Y.-W.; Lin, Y.; Liu, Z.; Kuo, H.-C. Dual Role of Quantum Dots as Color Conversion Layer and Suppression of Input Light for Full-Color Micro-LED Displays. *J. Phys. Chem. Lett.* **2021**, *12*, 6946–6954. [[CrossRef](#)] [[PubMed](#)]
25. Huang, C.-C.; Chu, K.-H.; Sher, C.-W.; Lin, C.-L.; Su, Y.-K.; Sun, C.-W.; Kuo, H.-C. High Stability of Liquid-Typed White Light-Emitting Diode with Zn<sub>0.8</sub>Cd<sub>0.2</sub>S White Quantum Dots. *Coatings* **2021**, *11*, 415. [[CrossRef](#)]
26. Lee, T.-Y.; Chung, S.-R. High Stability of Perovskite CsPbBr<sub>3</sub> Quantum Dots-Based White Light-Emitting Diodes. In Proceedings of the Physical Chemistry of Semiconductor Materials and Interfaces XIX, Online, 24 August–4 September 2020; pp. 8–17.

27. Lin, C.-H.; Kang, C.-Y.; Verma, A.; Wu, T.; Pai, Y.-M.; Chen, T.-Y.; Tsai, C.-L.; Yang, Y.-Z.; Sharma, S.; Sher, C.-W.; et al. Ultrawide Color Gamut Perovskite and CdSe/ZnS Quantum-Dots-Based White Light-Emitting Diode with High Luminous Efficiency. *Nanomaterials* **2019**, *9*, 1314. [[CrossRef](#)] [[PubMed](#)]
28. Lin, C.-H.; Verma, A.; Kang, C.-Y.; Pai, Y.-M.; Chen, T.-Y.; Yang, J.-J.; Sher, C.-W.; Yang, Y.-Z.; Lee, P.-T.; Lin, C.-C.; et al. Hybrid-Type White LEDs Based on Inorganic Halide Perovskite QDs: Candidates for Wide Color Gamut Display Backlights. *Photonics Res.* **2019**, *7*, 579–585. [[CrossRef](#)]
29. Hsu, S.-C.; Huang, Y.-M.; Huang, C.-P.; Lee, T.-Y.; Cho, Y.-Y.; Liu, Y.-H.; Manikandan, A.; Chueh, Y.-L.; Chen, T.-M.; Kuo, H.-C.; et al. Improved Long-Term Reliability of a Silica-Encapsulated Perovskite Quantum-Dot Light-Emitting Device with an Optically Pumped Remote Film Package. *ACS Omega* **2021**, *6*, 2836–2845. [[CrossRef](#)]
30. Tang, X.; Chen, W.; Liu, Z.; Du, J.; Yao, Z.; Huang, Y.; Chen, C.; Yang, Z.; Shi, T.; Hu, W.; et al. Ultrathin, Core–Shell Structured SiO<sub>2</sub> Coated Mn<sup>2+</sup>-Doped Perovskite Quantum Dots for Bright White Light-Emitting Diodes. *Small* **2019**, *15*, 1900484. [[CrossRef](#)]
31. Park, D.H.; Han, J.S.; Kim, W.; Jang, H.S. Facile synthesis of thermally stable CsPbBr<sub>3</sub> perovskite quantum dot-inorganic SiO<sub>2</sub> composites and their application to white light-emitting diodes with wide color gamut. *Dye. Pigment.* **2018**, *149*, 246–252. [[CrossRef](#)]
32. Xuan, T.; Huang, J.; Liu, H.; Lou, S.; Cao, L.; Gan, W.; Liu, R.-S.; Wang, J. Super-hydrophobic cesium lead halide perovskite quantum dot-polymer composites with high stability and luminescent efficiency for wide color gamut white light-emitting diodes. *Chem. Mater.* **2019**, *31*, 1042–1047. [[CrossRef](#)]
33. Geng, S.; Wen, Y.; Zhou, B.; Wang, Z.; Wang, P.; Jing, Y.; Cao, K.; Wang, K.; Chen, R. High Luminance and Stability of Perovskite Quantum Dot Light-Emitting Diodes via ZnBr<sub>2</sub> Passivation and an Ultrathin Al<sub>2</sub>O<sub>3</sub> Barrier with Improved Carrier Balance and Ion Diffusive Inhibition. *ACS Appl. Electron. Mater.* **2021**, *3*, 2362–2371. [[CrossRef](#)]
34. Yun, H.-S.; Noh, K.; Kim, J.; Noh, S.H.; Kim, G.-H.; Lee, W.; Na, H.B.; Yoon, T.-S.; Jang, J.; Kim, Y.; et al. CsPbBr<sub>3</sub> Perovskite Quantum Dot Light-Emitting Diodes Using Atomic Layer Deposited Al<sub>2</sub>O<sub>3</sub> and ZnO Interlayers. *Phys. Status Solidi (RRL)–Rapid Res. Lett.* **2020**, *14*, 1900573. [[CrossRef](#)]
35. Zhu, Y.; Liu, Y.; Ai, Q.; Gao, G.; Yuan, L.; Fang, Q.; Tian, X.; Zhang, X.; Egap, E.; Ajayan, P.M.; et al. In Situ Synthesis of Lead-Free Halide Perovskite–COF Nanocomposites as Photocatalysts for Photoinduced Polymerization in Both Organic and Aqueous Phases. *ACS Mater. Lett.* **2022**, *4*, 464–471. [[CrossRef](#)]
36. Cha, J.-H.; Noh, K.; Yin, W.; Lee, Y.; Park, Y.; Ahn, T.K.; Mayoral, A.; Kim, J.; Jung, D.-Y.; Terasaki, O. Formation and Encapsulation of All-Inorganic Lead Halide Perovskites at Room Temperature in Metal–Organic Frameworks. *J. Phys. Chem. Lett.* **2019**, *10*, 2270–2277. [[CrossRef](#)]
37. Pathiraja Mudalige Dona, S.T. Optimisation of Alumina Coating by Atomic Layer Deposition (ALD) Process as a Protective Scheme for CsPbBr<sub>3</sub> Perovskite Quantum Dots. Master’s Thesis, Lappeenranta University of Technology, Lappeenranta, Finland, 2018.
38. Lei, L.; Huang, D.; Chen, S.; Zhang, C.; Chen, Y.; Deng, R. Metal Chalcogenide/Oxide-Based Quantum Dots Decorated Functional Materials for Energy-Related Applications: Synthesis and Preservation. *Coord. Chem. Rev.* **2021**, *429*, 213715. [[CrossRef](#)]
39. Huang, Y.-M.; Ahmed, T.; Liu, A.-C.; Chen, S.-W.H.; Liang, K.-L.; Liou, Y.-H.; Ting, C.-C.; Kuo, W.-H.; Fang, Y.-H.; Lin, C.-C.; et al. High-Stability Quantum Dot-Converted 3-in-1 Full-Color Mini-Light-Emitting Diodes Passivated with Low-Temperature Atomic Layer Deposition. *IEEE Trans. Electron Devices* **2021**, *68*, 597–601. [[CrossRef](#)]
40. Sung, C.-H.; Huang, S.-D.; Kumar, G.; Lin, W.-C.; Lin, C.-C.; Kuo, H.-C.; Chen, F.-C. Highly Luminescent Perovskite Quantum Dots for Light-Emitting Devices: Photopatternable Perovskite Quantum Dot–Polymer Nanocomposites. *J. Mater. Chem. C* **2022**, *10*, 15941–15947. [[CrossRef](#)]
41. Zu, Y.; Xi, J.; Li, L.; Dai, J.; Wang, S.; Yun, F.; Jiao, B.; Dong, H.; Hou, X.; Wu, Z. High-Brightness and Color-Tunable FAPbBr<sub>3</sub> Perovskite Nanocrystals 2.0 Enable Ultrapure Green Luminescence for Achieving Recommendation 2020 Displays. *ACS Appl. Mater. Interfaces* **2019**, *12*, 2835–2841. [[CrossRef](#)]
42. Di Stasio, F.; Ramiro, I.; Bi, Y.; Christodoulou, S.; Stavrinadis, A.; Konstantatos, G. High-Efficiency Light-Emitting Diodes Based on Formamidinium Lead Bromide Nanocrystals and Solution Processed Transport Layers. *Chem. Mater.* **2018**, *30*, 6231–6235. [[CrossRef](#)]
43. Di Stasio, F.; Christodoulou, S.; Huo, N.; Konstantatos, G. Near-Unity Photoluminescence Quantum Yield in CsPbBr<sub>3</sub> Nanocrystal Solid-State Films via Postsynthesis Treatment with Lead Bromide. *Chem. Mater.* **2017**, *29*, 7663–7667. [[CrossRef](#)]
44. Loiudice, A.; Saris, S.; Oveisi, E.; Alexander, D.T.; Buonsanti, R. CsPbBr<sub>3</sub> QD/AlO<sub>x</sub> inorganic nanocomposites with exceptional stability in water, light, and heat. *Angew. Chem. Int. Ed.* **2017**, *56*, 10696–10701. [[CrossRef](#)]
45. Crisp, R.W.; Hashemi, F.S.M.; Alkemade, J.; Kirkwood, N.; Grimaldi, G.; Kinge, S.; Siebbeles, L.D.A.; van Ommen, J.R.; Houtepen, A.J. Atomic layer deposition of ZnO on InP quantum dot films for charge separation, stabilization, and solar cell formation. *Adv. Mater. Interfaces* **2020**, *7*, 1901600. [[CrossRef](#)]
46. Brennan, T.P.; Ardalan, P.; Lee, H.-B.-R.; Bakke, J.R.; Ding, I.-K.; McGehee, M.D.; Bent, S.F. Atomic Layer Deposition of CdS Quantum Dots for Solid-State Quantum Dot Sensitized Solar Cells. *Adv. Energy Mater.* **2011**, *1*, 1169–1175. [[CrossRef](#)]
47. Park, S.; Kim, B.J.; Kim, T.Y.; Jung, E.Y.; Lee, K.-M.; Hong, J.-A.; Jeon, W.; Park, Y.; Kang, S.J. Improving the Photodetection and Stability of a Visible-Light QDs/ZnO Phototransistor via an Al<sub>2</sub>O<sub>3</sub> Additional Layer. *J. Mater. Chem. C* **2021**, *9*, 2550–2560. [[CrossRef](#)]
48. Chen, Y.; Cai, J.; Lin, J.; Hu, X.; Wang, C.; Chen, E.; Sun, J.; Yan, Q.; Guo, T. Quantum-Dot Array with a Random Rough Interface Encapsulated by Atomic Layer Deposition. *Opt. Lett.* **2022**, *47*, 166–169. [[CrossRef](#)]

49. Wang, H.-C.; Bao, Z.; Tsai, H.-Y.; Tang, A.-C.; Liu, R.-S. Perovskite Quantum Dots and Their Application in Light-Emitting Diodes. *Small* **2018**, *14*, 1702433. [[CrossRef](#)]
50. Wang, Z.; Fu, R.; Li, F.; Xie, H.; He, P.; Sha, Q.; Tang, Z.; Wang, N.; Zhong, H. One-Step Polymeric Melt Encapsulation Method to Prepare CsPbBr<sub>3</sub> Perovskite Quantum Dots/Polymethyl Methacrylate Composite with High Performance. *Adv. Funct. Mater.* **2021**, *31*, 2010009. [[CrossRef](#)]
51. Zhang, Y.; Xiu, W.; Sun, Y.; Zhu, D.; Zhang, Q.; Yuwen, L.; Weng, L.; Teng, Z.; Wang, L. RGD-QD-MoS<sub>2</sub> nanosheets for targeted fluorescent imaging and photothermal therapy of cancer. *Nanoscale* **2017**, *9*, 15835–15845. [[CrossRef](#)]
52. Shim, J.-I.; Shin, D.-S.; Oh, C.-H.; Jung, H. Active Efficiency as a Key Parameter for Understanding the Efficiency Droop in InGaN-Based Light-Emitting Diodes. *ECS J. Solid State Sci. Technol.* **2019**, *9*, 015013. [[CrossRef](#)]
53. Zeferino, R.S.; Flores, M.B.; Pal, U. Photoluminescence and Raman scattering in Ag-doped ZnO nanoparticles. *J. Appl. Phys.* **2011**, *109*, 014308. [[CrossRef](#)]
54. Li, J.-S.; Tang, Y.; Li, Z.-T.; Li, J.-X.; Ding, X.-R.; Yu, B.-H.; Yu, S.-D.; Ou, J.-Z.; Kuo, H.-C. Toward 200 lumens per watt of quantum-dot white-light-emitting diodes by reducing reabsorption loss. *ACS Nano* **2020**, *15*, 550–562. [[CrossRef](#)]
55. Mei, S.; Liu, X.; Zhang, W.; Liu, R.; Zheng, L.; Guo, R.; Tian, P. High-Bandwidth White-Light System Combining a Micro-LED with Perovskite Quantum Dots for Visible Light Communication. *ACS Appl. Mater. Interfaces* **2018**, *10*, 5641–5648. [[CrossRef](#)] [[PubMed](#)]